Design of a Portable Alpha Detector for a Radiation Triage Mask

2011 Anthony J MacKay Student Paper Contest Winner

by Lenora Makin & Chad Shew
University of Ontario Institute of Technology

Background

A radiation triage mask (RTM) is a portable field device equipped with radiation detection capabilities. This device would be used in health risk or terrorist threat scenarios where a radiological dispersal device (RDD) could be detonated and a population could be at risk of receiving radioactive particulate deposition, both internally and externally. Through the installed Geiger–Müller (GM) counter and gamma spectroscopy detectors, an RTM is capable of detecting alpha, beta, and gamma radiation. However, the RTM has very limited efficiency detecting alpha particles due to their short range in air. The aim of this project is to design and construct a dedicated alpha detector that can be incorporated into an existing RTM.

The ultimate need for alpha detection capabilities in an RTM would be in the event that an RDD containing an alpha emitter were detonated. The alpha-emitting radionuclides most likely used in an RDD are Am-241, Cf-252, Po-210, Pu-238, or Ra-226. Alpha radiation particles cannot penetrate the dead layer of skin, however, if inhaled, the particles irradiate the lining of the lungs. Because of their high linear energy transfer (LET), inhaled alpha radiation particles can cause direct damage to the critical targets of cells (Giaccia & Hall, 2006).

Detection of particulate on the face indicates that there is deposition in the lungs. This is represented quantitatively by what is known as the orofacial-to-lung (OL) ratio. For the purposes of an RTM alpha detector, this ratio is assumed to be 10% (Sangwan, Burak & Gerald, 2003). That is, we assume 10% of the alpha activity present in the lungs will be present on the orofacial region. In the following section, we use the OL ratio to determine a target minimum detectable activity for the alpha detector.

Table 1: Orofacial Detectable Activity Dependent on Dose for Pu-2

	DCF(F) =1.1 × 10-1 mSv/Bq		DCF(M) =4.6 × 10-2		DCF(S) = 1.6 × 10-2	
Dose (mSv)	**Intake**	**OF Activity**	**Intake**	**OF Activity**	**Intake**	**OF Activity**
1*	9.09	0.91	21.74	2.17	62.50	6.25
2	18.18	1.82	43.48	4.35	125.00	12.50
3	27.27	2.73	65.22	6.52	187.50	18.75
5	45.45	4.55	108.70	10.87	312.50	31.25
10	90.91	9.09	217.39	21.74	625.00	62.50
20	181.82	18.18	434.78	43.48	1250.00	125.00
50	454.55	45.45	1086.96	108.70	3125.00	312.50
100	909.09	90.91	2173.91	217.39	6250.00	625.00

* **DCF Source:** *ICRP Publication 72: Age-dependent Doses to the Members of the Public from Intake of Radionuclides*, Part 5: Compilation of Ingestion and Inhalation Coefficients, Table A.2: Inhalation Dose Coefficients (Values for Adults).

Determination of Target Minimum Detectable Activity

An RTM alpha detector is designed to detect alpha activity on the face that corresponds to a 50 mSv lung dose. As stated earlier, the OL ratio assumes that the detectable activity on the face is 10% of the activity in the lungs. Therefore this ratio can be used to determine the detector's target activity, as shown below:

$$Lung\ Activity = L_A = Intake(Bq) = \frac{Dose(mSv)}{DCF(mSv/Bq)}$$

$$Orofacial\ to\ Lung\ Ratio = OL_A = \frac{Orofacial\ Activity}{Lung\ Activity}$$

$$= \frac{OF_A}{L_A} \cong 10\%$$

$$OF_A = OL_A \times Intake$$

DCF Source: *ICRP Publication 72: Age-dependent Doses to the Members of the Public from Intake of Radionuclides*, Part 5: Compilation of Ingestion and Inhalation Coefficients, Table A.2: Inhalation Dose Coefficients (Values for Adults).

Table 1 illustrates that a worst-case-scenario lung dose of 50 mSv corresponds to 45 Bq activity on the orofacial region. Thus, the alpha detector should be able to determine the presence of at least 45 Bq of alpha activity.

Design of the Detector

In this section, we provide the design of our RTM ZnS(Ag) Scintillator Alpha Detector. This is followed by a theoretical analysis of the detector performance, and then the supporting laboratory results. A basic overview of the detector setup and its expected use are also provided in this section. Justification for our component choice, placement, and integration are provided in the performance analysis section.

As seen in Figure 1, the detector consists of a series of components integrated sequentially into the RTM side panel. The face-end of the RTM side panel becomes the detector window, through which alpha particles pass. A protective steel mesh covers the detector window. Directly behind the mesh is an ultrathin layer of aluminized Mylar (thickness of approximately 2 µm). There is a thin (60 µm) layer of ZnS(Ag) crystalline scintillator powder immediately following the Mylar film. This powder layer is applied directly to a thin layer of Lucite using optically transparent double-sided tape (not shown on schematic). The Lucite layer is then followed by a 2 cm air gap, enclosed on the top, bottom, and sides by plane mirrors. The back side of the air gap leads directly to the PMT, which extends another 4 cm toward the front panel of the RTM. The PMT signal cable (not shown) extends from the base of the PMT and connects to the RTM's electronics in the front panel.

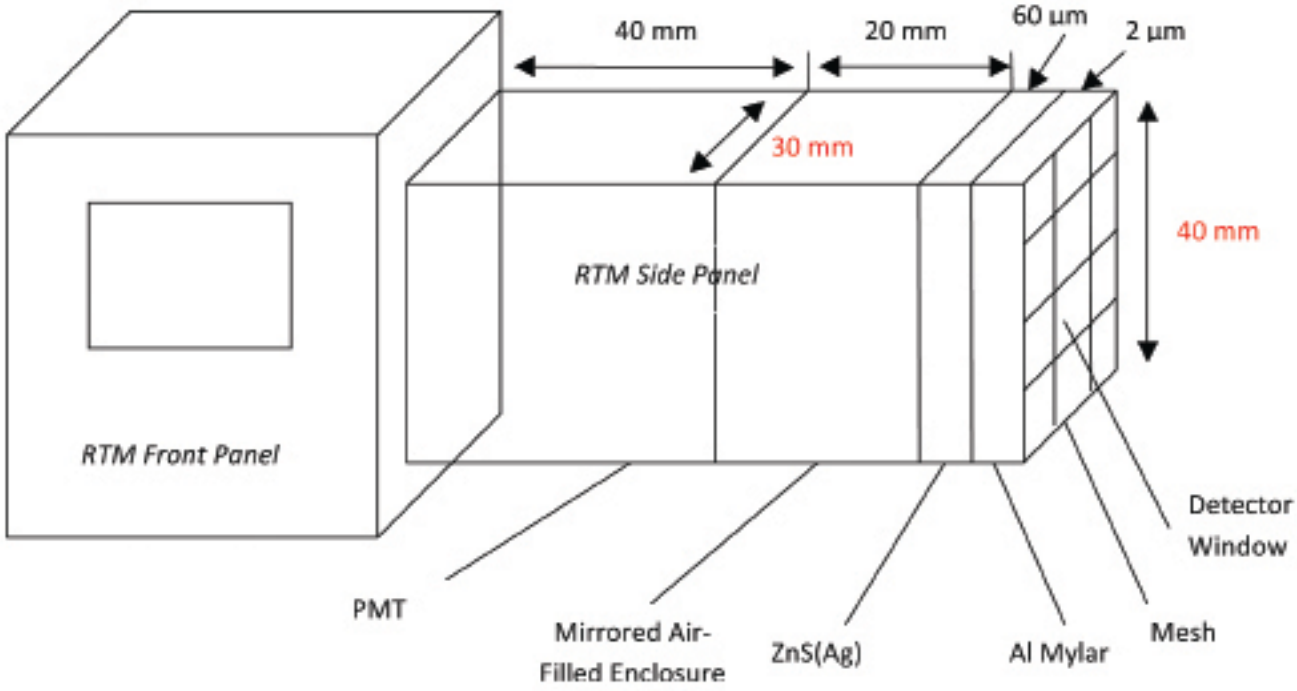

Figure 1: Detector Assembly Overview Schematic (not to scale)

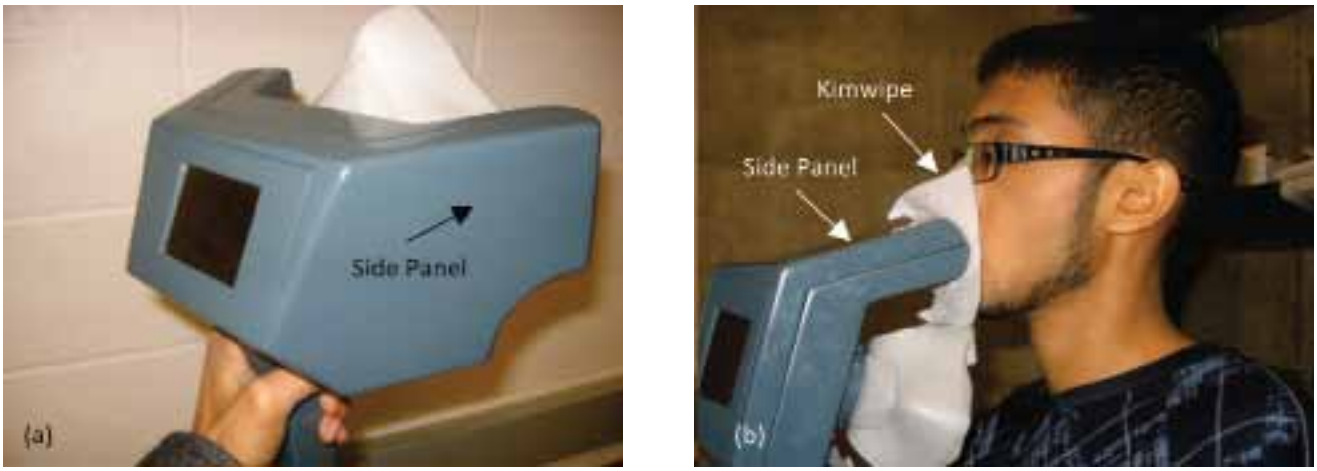

Figure 2: (a) RTM Upright View (b) RTM (side view) in operation for Alpha Detection

As seen in Figure 2(b), the detector window is designed to be in contact with a Kimwipe, which is then in contact with the individual's face. In other words, the Kimwipe lies between the detector and the individual's face. Light pressure is applied to the RTM handle to hold the Kimwipe in place against the face and to eliminate unnecessary air gaps. The detector window encompasses an area of approximately 12 cm^2, which is enough to cover a large portion of an average person's orofacial region (Tilley, 2002).

Analysis of Theoretical Performance

What follows is a simulation of the detector's efficiency. A starting activity of 45 Bq was chosen based on previous calculations. Performance of each detector component is handled sequentially—energy, light, and count losses due to each component are all taken into account. A conservative approach is used where possible to avoid overestimation of the efficiency.

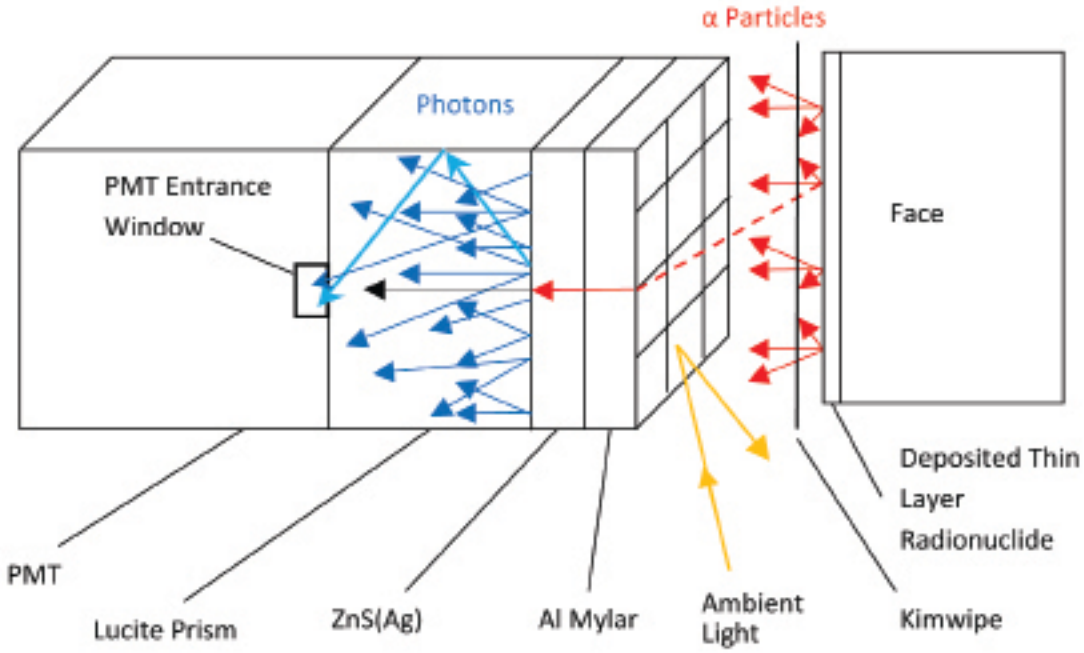

Figure 3: Sequence of Interactions in Detector (not to scale)

In the event of radioactive dispersal, it is assumed a thin layer of alpha-emitting radionuclide will be deposited on an individual's face. The activity of the radionuclide is assumed to be low (≈ 45 Bq), however it could potentially be spread over a large area. Thus, it is essential to maximize the surface area of the detector in order to maximize detectable activity. For this reason, a detector surface area of 12 cm^2 was chosen. It should also be noted that the deposited particulate layer is assumed to be sufficiently thin, such that minimal self-absorption of alpha particles occurs.

As shown above, alpha particles may be emitted over 180 degrees from numerous points on the orofacial area. This results in a diffuse spread of alpha particles away from the face. Since the other 180 degrees (pointed toward the face) represents lost (undetectable) alpha particles, we can immediately state the following:

$$Surface\ Emission\ Rate\ [2\pi] = 0.5{\times}45\ Bq \approx 22\ Bq$$

As stated previously, a Kimwipe is to be placed between the face and the detector window. Empirically, it was found that a standard Kimwipe attenuates a source of alpha particles by approximately 50%. This measurement assumes essentially no air gap between the face, Kimwipe, and detector window. Such an assumption is valid, since the detector should be pressed lightly against the Kimwipe (as seen in Figure 2).

$$\alpha/s\ reaching\ detector\ window = 0.5{\times}22\ Bq \approx 11\ \alpha/s$$

The majority of the alpha particles reaching the detector window will pass through the mesh and the ultrathin Mylar film, however, some of the detector window surface area is taken up by the steel mesh.

A square unit of the mesh is shown below:

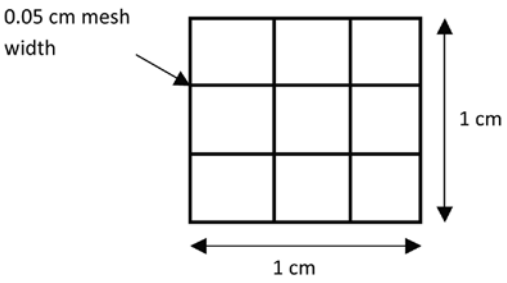

$$1\ mesh\ line = 0.05\ cm{\times}1\ cm = 0.05\ cm^2$$

$$Area\ of\ 4\ mesh\ lines = 4{\times}0.05\ cm^2 = 0.2\ cm^2$$

$$0.2\ cm^2/1\ cm^2 = 20\ \%\ area\ taken\ up\ by\ mesh$$

$$\alpha/s\ reaching\ Mylar\ film = (1-0.2){\times}11\ \alpha/s \approx 9\ \alpha/s$$

It can be assumed all alpha particles that reach the Mylar film will pass through the mesh, and some energy loss will occur. As a conservative measure, this is taken into account by reducing the incident alpha particle energy to 3 MeV from the average of ≈5 MeV at the source. This loss also accounts for any miniscule air gaps between the detector and face or between the Kimwipe layer and the detector. A loss of 2 MeV is roughly equivalent to a 2 cm air gap.

Aluminized Mylar was chosen to precede the ZnS(Ag) scintillator primarily due to its excellent light-blocking ability and its availability as an ultrathin film. Optimal density thickness for alpha penetration was found to be ≈ 0.25 mg/cm^2 (Vainblat et al., 2004). The Mylar density is 1.40 g/cm^2 (National Institute of Standards and Technology, 2010).

$$Optimal\ mylar\ thickness = t_\rho/\rho = 0.25{\times}10^{-3}/1.40 \approx 1.8\ \mu m$$

Upon passing through the Mylar film, the alpha particles encounter the crystalline ZnS(Ag) scintillator layer. The ZnS(Ag) layer must be sufficiently thin so as to not absorb its own scintillation light. Data show that loss of light becomes significant at density thicknesses greater than 25 mg/cm^2 (Knoll, 2000). The ZnS density is 4.9 g/cm^2 (Loyola University, 1992).

$$ZnS(Ag)\ thickness = t_\rho/\rho = 25{\times}10^{-3}/4.09 \approx 61.1\ \mu m$$

An individual alpha particle will promptly transfer its energy to the ZnS(Ag), resulting in emission of photons at a wavelength of 450 nm. The photon yield for ZnS(Ag) is ≈ 26,000 photons/MeV (Derenzo, Boswell & Brennan, 2010), which leads to the following:

$$photons/\alpha = photons/MeV \times \alpha\ Energy = 26{,}000{\times}3 = 78{,}000$$

As seen in figure 3, these photons will be emitted diffusely into a 24 cm^3 air gap. The top, bottom, and side boundaries of the air gap are plane mirrors. These mirrors promote reflection of photons toward the PMT target. Of the 78,000 photons, a large percentage will not reach the PMT entrance window. This light loss is due to the difference in size between the PMT entrance window and the ZnS(Ag) scintillator surface.

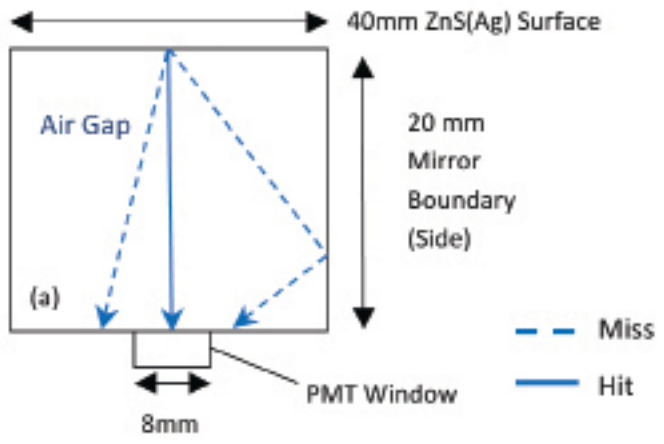

Figure 4: Potential Photon Paths (not to scale)

Figure 4 (on page 31) shows a two dimensional simulation of the emission of a few photons from the ZnS(Ag) surface. For this illustration, a single point along the ZnS(Ag) surface was chosen, from which only a few rays are emitted. It should be noted that light can be emitted along the entire ZnS(Ag) surface in three dimensions, and in any direction. If reflections are ignored and the photons are assumed to emit in all directions, the following calculation conservatively estimates the loss of light:

$$Light\ Collection\ Efficiency \cong \frac{Surface\ Area\ of\ PMT\ Window}{Surface\ Area\ of\ Sphere} = \frac{0.5\ cm^2}{50\ cm^2} = 1\%$$

$$\%\ light\ reaching\ PMT\ window = 1\ \%$$

$$photons\ reaching\ PMT\ window = 78{,}000 \times 0.01 = 780\ photons/\alpha$$

It is then useful to determine the energy of each photon:

$$Energy\ per\ photon = \frac{hc}{\lambda} = 6.626\times10^{-34}\ J\cdot s \times \frac{c\ \ m/s}{450\times10^{-9}\ m} \approx 4.4\times10^{-19}\ J/photon$$

This leads to a simple determination of the total incident photon energy per alpha particle:

$$total\ incident\ photon\ E = photons/\alpha\ \times\ J/photon \approx 3.4\times10^{-16}\ J/\alpha,$$

Combining this quantity with the rate of α particles striking the ZnS(Ag) produces the following yields:

$$Radiant\ Power\ Produced = 9\ \alpha/s\ \times (3.4\times10^{-16})\ J/\alpha \approx 3.1\times10^{-15}\ W = 3.1\times10^{-3}\ pW$$

Using the count sensitivity quoted for the chosen PMT (Hamamatsu, 2010), it is then possible to determine if any counts will not be registered:

$$Count\ Sensitivty \approx 3.1\times10^{-6}\ pW/cps$$

$$Radiant\ Power\ required\ to\ register\ 9\ cps = 9\times(3.1\times10^{-6}\ pW) = 2.8\times10^{-5}\ pW$$

$$3.1\times10^{-3}\ pW \gg 2.8\times10^{-5}\ pW\ \rightarrow 9\ cps\ registered$$

These equations indicate that the light output produced is still about 2 orders of magnitude larger than the radiant power required. This is primarily due to two major factors: (1) the chosen PMT sensitivity exceeds the requirement, and (2) the light output of ZnS(Ag) is relatively high. Taking all the aforementioned factors into consideration, it is finally possible to determine the efficiency of the Portable Alpha Detector.

$$\boldsymbol{Efficiency = 20\%}$$

Table 2: Percentage Count Losses due to Individual Component

Sequence	Component/ Factor	% Loss	% Remain	α/s
0	Thin-Layer Source	0	100	45
1	180° Absorption	50	50	22
2	Kimwipe	50	25	11
3	Steel Mesh	20	20	9
4	Light Loss/ PMT	0	20	9

Experimental Results

The RTM alpha detector was used in the laboratory to count small Po-210 and Am-241 disk sources. The Po-210 was approximately 4 mm in diameter and had an activity of 72 Bq, and the Am-241 was approximately 4 mm in diameter with an activity of 33 kBq. Each counting run was performed for only ten seconds to simulate the speed of counting in a field application. It should be noted that due to the high light sensitivity of the PMT, the counts obtained were significantly higher than the activity of the sources. That is, for each alpha particle that interacted with the detector, enough light was produced to result in multiple counts. This phenomenon is taken into account by following calculation:

$$Count\ Sensitivity = 3.2\times10^{5}\ s^{-1}\ pW^{-1}$$

$$Radiant\ Power\ per\ Alpha\ Particle\ (RPA) = 3.4\times10^{-14}\ J/\alpha\ \times 1\ \alpha/s = 3.4\times10^{-2}\ pW$$

$$Incident\ Radiant\ Power\ per\ Alpha\ Particle\ (IRPA) = RPA\times Light\ Collection\ Efficiency$$

$$IRPA = (3.4\times10^{-2}\ pW)\times0.01 = 3.4\times10^{-4}\ pW$$

$$Counts\ per\ \alpha\ Particle = IRPA\times Count\ Sensitivity = (3.4\times10^{-4}\ pW)\times(3.2\times10^{5}\ s^{-1}\ pW^{-1})$$

$$\boldsymbol{Counts\ per\ Alpha\ Particle\ (CPA) \cong 110}$$

The dark counts associated with the electrical noise of the PMT must also be considered. These are the counts that the PMT will register when no source is present. They must be subtracted from the gross counts because they are not generated by the source. The dark counts were measured in the laboratory after storing the PMT in darkness for 30 minutes. With no source present near the detector, the dark counts were found to be

Table 3: Counting Results Averaged for Five 10-Second Counts with Two Different Sources

Nuclide	Gross Counts	Net Counts	Real Counts (10s)	Activity (Bq)	Efficiency (%)
Po-210	20300 ± 640	12300 ± 640	112 ± 6	72	16
Am-241	6299000 ± 6800	6291000 ± 6800	57190 ± 60	33200	17

800 ± 2 cps. It should be noted that the dark counts did not vary significantly, and therefore they could be reliably subtracted from the gross counts.

Results were obtained by performing five 10-second counts with each source placed over the detector. The averaged results of the counting for the two sources are shown in Table 3 (on page 32). The Gross Counts column shows the total counts registered by the detector. Net Counts refers to the counts after the dark counts have been subtracted. The Real Counts are reported by dividing the Net Counts by the Counts per Alpha Particle (CPA), as determined above.

Conclusion

It is of interest to note that a very large portion of the count losses are due to the external geometry of the counting. That is, the intrinsic efficiency of the detector is expected to be very high. It should also be noted that the theoretical calculated efficiency is highly dependent on the thickness of the deposited layer of radionuclide. This explains why the efficiency found in the counting experiments is lower than the theoretical efficiency. A thin deposited layer with a large surface area would be detected with a higher counting efficiency than the disk sources used in the experiments. This is because the large surface area of the detector favours a thin layer as opposed to a point source. In addition, for a thin layer there would be less self-absorption of alpha particles, which would further increase the counting efficiency.

In the event of radioactive dispersal, the radionuclide can be modeled to exist as a thin layer on the face. In reality, the layer may not be of uniform thickness, but it is still likely to be thinner than the disk sources used in the laboratory. Thus the detector would be expected to perform with greater efficiency in the field than in the laboratory tests.

Even considering the lowest obtained efficiency (16%), the detector is still able to achieve its target detectable activity. For an intake leading to a 50 mSv dose, the orofacial activity is estimated at 45 Bq and experimental results indicate that the detector would register 7 cps (420 cpm). Therefore, in the event of a dispersal of radioactivity, the detector is expected to be more than capable of determining the presence and relative activity of an alpha-emitting radionuclide.

References

Cember, H. (1996). *Introduction to Health Physics* (3rd ed.). New York: The McGraw-Hill Companies.

Derenzo, S., Boswell, M., & Brennan, K. (2010, October 25). *Scintillation Properties*. Retrieved November 27, 2010, from http://scintillator.lbl.gov.

Giaccia, A. J. & Hall, E. J. (2006). *Radiobiology for the Radiologist* (6th ed.). Philidelphia: Lippincot Williams & Wilkins.

Hamamatsu. (2010). *Photon Counting Head H10682 Series*. Japan: Hamamatsu Photonics K. K.

Knoll, G. F. (2000). *Radiation Detection and Measurement*. Hoboken: John Wiley & Sons Inc.

Loyola University. (1992). *Interactive Materials*. Retrieved November 25, 2010, from http://www.luc.edu/faculty/spavko1/minerals/zns/zns-main.htm.

National Institute of Standards and Technology. (2010, October 5). *Composition of Polyethylene Terephthalate (Mylar)*. Retrieved November 25, 2010, from http://physics.nist.gov/cgibin/Star/compos.pl?matno=222.

Sangwan, S., Burak K., G., & Gerald C., S. (2003, October 21). Facemasks and Facial Deposition of Aerosols. *Pediatric Pulmonology, 37*(5), pp. 447-452.

Tilley, A. R. (2002). *The Measure of Man & Woman: Human Factors in Design* (Revised edition). New York: John Wiley & Sons Inc.

Vainblat et al. (2004). Determination of Parameters Relevant to Alpha Spectrometry when Employing Source Coating. *Applied Radiation and Isotopes, 61*, pp. 307-311.

Leah Shuparski Catches Up With This Year's Student Paper Contest Winners

. . . continued from page 27

LM: My favourite part of the conference was right after I finished presenting. I got to feel like an expert for 10 minutes and tell everyone about the hard work and research we had done at UOIT. That was pretty satisfying. I also agree with Chad that the banquet was a definite highlight of the week.

Your interview will be read by most of the CRPA membership. Is there anything you'd like to say to them?

CS: I would like to give my sincerest thanks to the members and organizers for putting on a great conference, and for keeping CRPA at the forefront of the industry. I would also like to encourage continued support and interest in student initiatives.

LM: Thank you! I really enjoyed myself at the conference, and I definitely encourage them to keep striving for student involvement. My warmest regards to the organizers and members for participating.